International Journal of Ventilation

ISSN: 1473-3315 (Print) 2044-4044 (Online) Journal homepage: http://www.tandfonline.com/loi/tjov20

The Impact of Urban Wind Environments on Natural Ventilation

Erdal Turkbeyler, Runming Yao, Rosario Nobile, Tom Bentham & David Lim

To cite this article: Erdal Turkbeyler, Runming Yao, Rosario Nobile, Tom Bentham & David Lim (2012) The Impact of Urban Wind Environments on Natural Ventilation, International Journal of Ventilation, 11:1, 17-28, DOI: 10.1080/14733315.2012.11683967

To link to this article: http://dx.doi.org/10.1080/14733315.2012.11683967

Published online: 29 Mar 2016.

The Impact of Urban Wind Environments on Natural Ventilation

Erdal Turkbeyler[1, 2], Runming Yao[1], Rosario Nobile[1], Tom Bentham[3], David Lim[1]

[1]School of Construction Management and Engineering, The University of Reading, Whiteknights, PO Box 219, Reading, RG6 6AW, United Kingdom
[2]Department of Mechanical and Automotive Engineering, Coventry University, Priory Street, Coventry, CV1 5FB, United Kingdom;
[3]Max Fordham LLP, 42 Gloucester Crescent, London, NW1 7PE, United Kingdom

Abstract

The aim of this paper is to illustrate the impact of urban wind environments when assessing the availability of natural ventilation. A numerical study of urban airflow for a complex of five building blocks located at the University of Reading, UK is presented. The computational fluid dynamics software package ANSYS was used to simulate six typical cases of urban wind environments and to assess the potential for natural ventilation. The study highlights the impact of three typical architectural forms (street canyons, semi-enclosures and courtyards) on the local wind environment. Simulation results were also compared with experimental data collected from six locations on the building complex. The study demonstrates that ventilation strategies formed using regional weather data may have a propensity to over-estimate the potential for natural ventilation and cooling, due to the impact of urban form which creates a unique microclimate. Characteristics of urban wind flow patterns are presented as a guideline and can be used to assess the design and performance of natural or hybrid ventilation and the opportunity for passive cooling.

Key words: buildings, CFD simulation, natural ventilation, urban airflow, urban building layout, wind.

1. Introduction

As the practice of sustainable architecture becomes mandatory in many cases within the United Kingdom and elsewhere (CLG, 2006), there is an increasing imperative to reduce emissions associated with ventilation and cooling. In addition to the environmental agenda, natural ventilation hugely improves indoor air quality and reduces the potential for cases of sick building syndrome (Rostron, 1998). Also, it is associated with increasing the psychological wellbeing of occupants. Building service strategies which integrate natural ventilation, hybrid ventilation or passive cooling technology within the overall concept rely heavily on data pertaining to regional climate, in particular prevailing wind, average flow rates and direction. However, it is known that the built form significantly impacts on *general* airflow characteristics, creating a microclimate that can produce unexpected outcomes; namely, under-performing ventilation systems, uncomfortable indoor environments and windy public spaces at street level.

The urban wind environment is one of the most important factors that affect occupant health, outdoor and indoor thermal comfort, air quality and the energy performance of buildings (Yang, 2011; Memon and Leung, 2010; Priyadarsini *et al* 2008). Urban form has a significant impact on urban wind patterns. Understanding the relationship between built form and urban wind pattern is important to better understand the cooling and ventilating effects of urban wind. For example, this is important when analysing the cooling effect of wind, particularly during the night, to help mitigate the adverse effects of an urban heat island on occupant thermal comfort, both indoors and outdoors. Additionally, a favourable urban wind pattern indirectly contributes to the reduction of carbon dioxide emissions, as passive indoor ventilation reduces the need for mechanical air conditioning (Kolokotroni, 2006; Fung et al, 2006). Moreover, air pollution in the urban environment is best reduced by ventilation in the form of an uniform urban wind distribution (Vaughan, 2002; Zhang et al, 2011).

For assessing the potential of natural ventilation for a building configuration, the URBVENT project (Ghiaus and Allard et al, 2005) developed simple methodologies that considered air temperature, noise and air pollution. They considered only stack induced flow (i.e. in the absence of wind) for developing a database for the natural ventilation capacity of a building configuration, because the pressure coefficients of wind effect were not available. The URBVENT project also studied the wind effect for street canyon configurations. However, they restricted the wind pattern in a street canyon to only three wind directions: parallel, perpendicular and oblique winds. The present work aims to investigate any urban wind pattern in three urban forms, the street canyon, semi-closure and courtyard.

When CFD analysis is conducted on a building's wind flow characteristics, it provides detailed and spatially continuous information on the resulting urban wind pattern. This information is vital for the assessment of design and performance features, such as pedestrian comfort, façade design, positioning of air intakes and exhausts, distribution of contaminants throughout a site and its surroundings, and building energy requirements for heating and cooling loads.

In recent years, experimental studies have been conducted on the urban microclimate of a low-rise building complex in Reading (Turkbeyler and Yao, 2009) and a mixture of medium and high-rise buildings in London (Turkbeyler et al, 2011). They conducted their study by measuring microclimatic variables (wind speed and direction) at six strategic locations within these building complexes between the urban canopy and roof-top level. Their measurements show that the building's layout and orientation significantly effects the temporal and spatial distribution of microclimatic variables. In addition, the experimental study has also shown that a building's measured microclimatic variables, including air temperature, wind speed and direction can be considerably different from the reported local and regional meteorological weather. By nature, the experimental measurement locations of microclimatic variables were limited in terms of number; six locations for Reading and six for London.

To better understand the continuous spatial relationship between urban form and the resulting urban wind patterns, a CFD analysis of urban airflow was carried out for the building complex at Reading. This building complex presents different built forms including a street canyon, a courtyard-like area and a semi-enclosure. The objective was to conduct a detailed investigation of the affect of layout and orientation of buildings on the spatial distribution of urban wind patterns. To achieve these objectives, CFD simulations were carried out for the principal wind directions observed during the experimental study. Flow simulations were conducted using ANSYS software and the results are presented and the implications discussed. A brief comparison between the simulation results and the experimental measurements are also presented.

Before reviewing the literature on previous CFD simulations, it is worth noting the three types of wind flow with respect urban form. The literature (Oke, 1988) identifies these as: (i) isolated roughness flow; (ii) wake interference flow; and (iii) skimming flow. The principle characteristic determining flow type is the ratio of building height (H) to the distance (W) between building arrays, as in the case of urban street canyons. If the ratio (H/W) of buildings, along the direction of the approaching flow is less than approximately 0.30, the flow is classified as isolated roughness flow where the building interacts with the approaching wind in isolation without any effects on downstream building. For a cube shaped building, about two-thirds of the approaching mass flow-rate flows around the sidewalls and the remaining third flows over the roof causing a turbulent 'corner flow' effect. Another characteristic of isolated roughness flow, is faster airflow along the sidewalls and over the roof which may lead to the 'venturi effect' if buildings in the lateral direction are in close proximity. The diverted side and roof flows eventually separate from the building surfaces creating a low-speed wake flow. Downstream of the building, the flow meets ground level and eventually increases to the speed of the surrounding airflow. When the building density increases in the direction of the airflow, and the ratio (H/W) of a street canyon increases (between 0.30 and 0.70), this wake flow interferes with the flow of downstream buildings. This is known as 'wake interference' flow. Air pollution ventilation between the building arrays may be adversely affected by this building spacing. Finally, if the buildings become too close (H/W ratio > 0.7), the roof flow is forced to skim over the downstream building roofs without ventilating the air pollution between the buildings. This is known as 'skimming' flow. In this case, a stable vortex appears in the street canyon between building rows. However, if the approaching wind makes an oblique angle with the axis of the street canyon, the vortex moves along the street canyon axis in a cork-screw motion (Nakamoura and Oke, 1967)

Unlike a street canyon, a general urban layout creates different levels of resistance to airflow at different locations due to their different shapes, sizes and layout. As a result, the interaction of urban wind patterns and the city layout becomes more complicated than these archetypal flows. Therefore, it becomes imperative to investigate urban wind patterns in terms of different built forms of city structures, such as street canyons, semi-enclosures, courtyards and open spaces (Serteser and Ok, 2009). Even then, there is interaction between the wind patterns generated by each of these urban structures as they collectively shape the urban form.

Microclimatic field measurements, within urban forms, have been shown to be useful for monitoring the wind speed and direction at certain key site locations, but the information they provide for the microclimatic wind pattern is limited due their discrete nature. However, the analysis of urban wind environments can be carried out by CFD simulation or by using wind tunnel testing on scale models. Urban planners require detailed wind data in the initial design stages for assessing planning concepts in order to identify problems associated with the wind environment on buildings, public spaces and streets.

Chen (2004) compared CFD simulations of building complexes against other design tools to account for the impact of wind in architectural design. In this study, CFD was the preferred method when compared with other tools including model mock-ups, wind tunnels, and nodal models, as it appeared the most affordable, accurate, and informative method. Similarly, Jiang et al (2007) used CFD simulation as a robust method for analysing airflow around buildings as well as assessing natural ventilation in buildings. They showed that a preliminary site design could be modified, following CFD simulation, to reduce wind chill effects for pedestrians during winter months. This was realized by managing the building array to compensate for prevailing north winds by creating a sheltering effect for the overall building complex. However, the relationship between different built forms and wind directions was not studied.

2. Numerical Method

2.1 Description of the Building Complex

CFD simulations were performed for a building complex at the Whiteknights campus, University of Reading, UK (long. $51^{o}\ 26^{'}$ N, lat. $0^{o}\ 56^{'}$ W). The complex comprises six buildings, labelled Building *A* to *F* in the aerial photograph below (Figure 1) which shows the general urban form, verges and foliage. Building dimensions and orientations are given in Table 1. All building roofs are pitched except building *A* which has a flat roof. Figure 2 shows the data instrument points 1 to 6 on the master site plan. The buildings create different

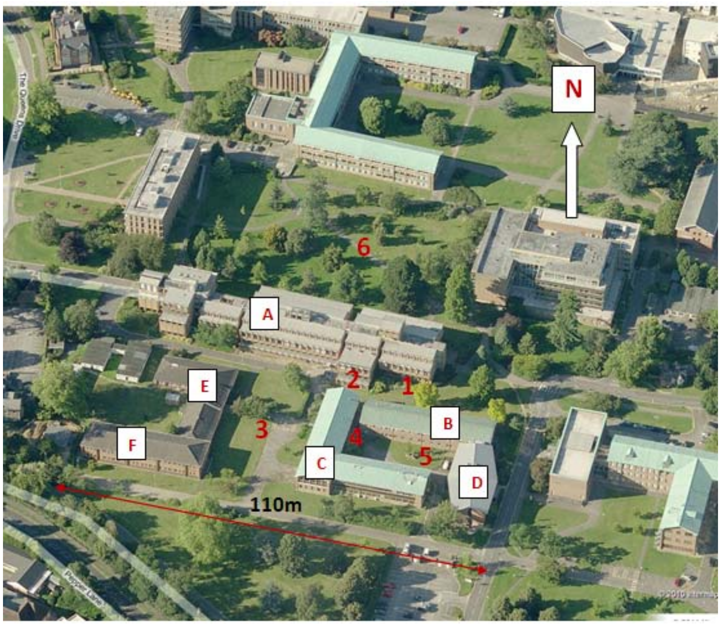

Figure 1. Aerial photograph of the Reading building complex.

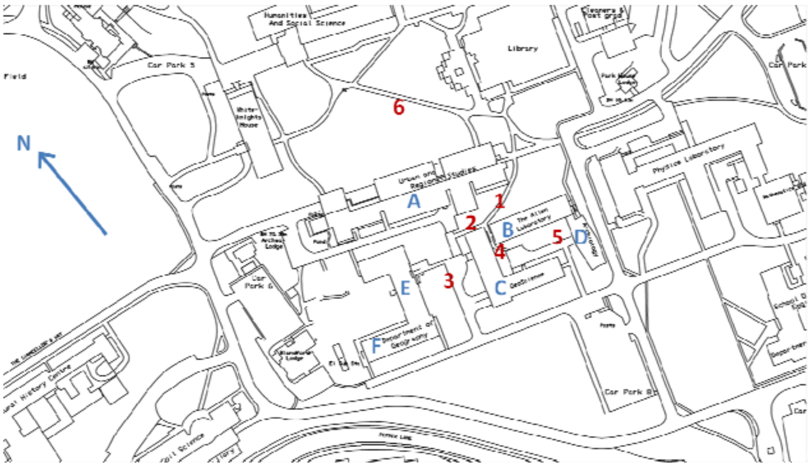

Figure 2. Site plan showing data instrument locations 1 to 6, and buildings A to F (scale 1:2000).

Table 1. Description of Building Complex.

Building	**Dimensions** L(m), D(m) and H (m)	**Orientation** (angle of east wall normal from the north axis)	**Material**
Building A	121, 27, 12	107.5^0 clockwise	Concrete
Building B	50, 13, 9.5	107.5^0 clockwise	Brick
Building C	48, 13, 9.5 (S-N) 34, 13, 9.5 (W-E)	107.5^0 clockwise 107.5^0 clockwise	Brick
Building D	35, 15, 9.5	90^0 clockwise	Brick
Building E	45, 17, 5.5	107.5^0 clockwise	Brick
Building F	44, 14, 9.5	107.5^0 clockwise	Brick

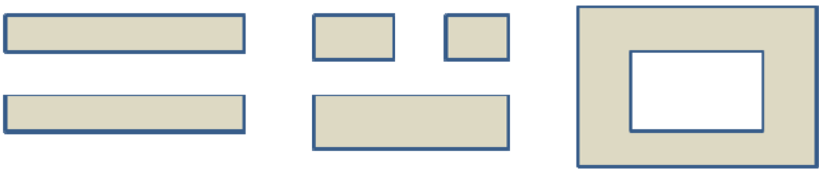

Figure 3. Three common architectural built forms.

urban forms: buildings *A* and *B*, and buildings *A* and *E* form a street canyon; buildings *A*, *B*, *C*, and *E* reflect a semi-enclosure; and buildings *B*, *C* and *D* create a courtyard-like form. The street canyon (axis east south east) is oriented clockwise from the east-west axis by an angle of 17.5°. Schematic representations of the three typical urban forms are illustrated in Figure 3.

2.2 Simulation Cases

In order to investigate the characteristics of urban wind patterns within the building complex, airflow around the buildings was simulated for six wind directions (four cardinal and two inter-cardinal: N, E, S, W, NE, SW) shown in Table 2. It is assumed that the inclusivity of the aforementioned wind

Table 2. Simulation case specifications.

Simulation case	Local Wind Direction	Local Wind Speed at 10m	Experimental Date	Experimental Time
1	South - (S)	4.0 m/s	6 April 2009	2pm
2	North - (N)	4.0 m/s	30 November 2009	12pm
3	East – (E)	4.5 m/s	7 March 2010	11am
4	West – (W)	6.0 m/s	23 November 2009	15pm
5	North East- (NE)	4.0 m/s	12 December 2009	12pm
6	South West (SW)	4.0 m/s	28 November 2009	8am

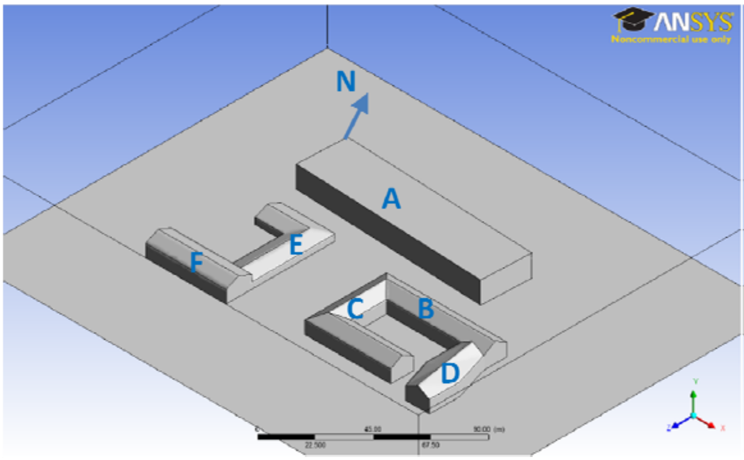

Figure 4. Simulated building complex.

directions is suitable for the level of analysis. Specific data entries (recording instantaneous wind direction, speed, date and time) were extracted from the complete experimental dataset, to correspond with the six chosen wind directions. For each of the six analysis wind directions, the data entry which recorded the greatest wind speed (and corresponding date) was selected in order to develop simulation wind pattern characteristics. The value of the measured wind speed, recorded at 10 m above ground level, was used as the input value. The approaching wind profile at the inlet boundaries were calculated in accordance with the logarithmic distribution of wind speed with height. This is zero at ground level. For the simulated building site (Figure 4), the experimental wind profile was imposed at the computational domain inlet flow boundaries.

2.3 Simulation Specifications

This section details the simulation parameters and associated methods. The ANSYS CFX 12.0 software package was used to implement all simulations. The solid model of the buildings was generated with ProEngineer 4.0 and imported into ANSYS CFX 12.0 (Figure 4). The computational domain, upstream and downstream extensions were set to 48 m which was four times the height of the tallest building (building *A* – 12 m). The same margin was added to the sides of the building complex. The ratio of the frontal area of the complex to the approaching flow area of the CFD domain leads to a flow blockage ratio of approximately 13%. The computational mesh was generated by adopting the Tetrahedrons Method due to the geometry of the buildings, with a total of 1.1×10^6 elements. The mesh around the buildings, which forms the wake development region, was refined through the use of the facing sizing and inflation options available in ANSYS 12.0. Here, the use of prism elements was able to capture boundary layer effects more effectively and efficiently.

A steady state mode with a constant wind speed profile at the inlet was considered for all numerical simulations which used the Shear Stress Transport

(SST) turbulence model. The number of interactions in the solver control was set to 200 steps and the residual accuracy for the Root Mean Square (RMS) was 1.0 e^{-4}. At the flow boundaries, the following conditions presided: steady velocity at the inlet with a logarithmic profile; standard atmospheric pressure at the exit and the top of the fluid domain; and standard wall conditions for all the surfaces of the buildings and ground. The simulation model only features buildings *A* to *F*, excluding neighbouring buildings which occupy the extended area in reality (Figure 4). Another modelling simplification occurs with site orientation, whereby the simulated X-Z axes do not exactly coincide with true east and west. The simulated X axis is 17.5^o east south east and the Z axis 17.5^o south south west. The average time for each complete simulation was approximately 40 minutes, performed using a Dell T5500 PC (specification: Intel(R) Xeon(R) CPU X5570 at 2.93 GHz, 24GB RAM, 64-bit Operating System).

3 Results and Discussion

Figures 5 to 10 illustrate the numerical results of the six simulation cases, showing velocity vectors at a height of 4 m above ground level to reflect the height of the weather data instruments. This height is 33% of the height of building *A*, 42% of buildings *B*, *C*, *D*, and *F* and 72% of building *E*. The following notation is used: e.g. an urban street canyon created by building *X* and building *Y* is described as canyon *XY*. Later, the simulation results are also displayed on some 2D vertical cross-sectional planes at certain locations of the building complex.

3.1 Simulation Case 1: Southerly Wind (S)

The interaction between buildings *A* – *F* and the prevailing south wind results in distinct airflow features at different locations. With respect to air temperature distributions within the same building complex (Turkbeyler and Yao, 2009), the urban wind pattern shows a higher degree of microclimatic variation. The observed features of this urban wind pattern (Figure 5) include:

a) Channelling wind along the passage between buildings *C* and *E*, which is virtually parallel to the prevailing wind direction;

b) Blockage and diversion of the channelled wind by building *A*, forcing the wind to divert down two urban street canyons *AE* and *AB;*

c) The flow in the street canyon AE is faster than the flow in the street canyon *AB*. This may be caused by three factors: (i) the oblique angle of the channelled flow with respect to building *A*, favouring street canyon *AE*; (ii) street canyon *AE* is narrower than street canyon *AB*, causing greater wind speeds along *AE*; (iii) the height of building *E* (5.5 m) is less than building *B* (9.5 m), thus presenting lower resistance to the prevailing wind;

d) Buildings *C*, *D* and *F* block the prevailing wind causing faster corner flows at these buildings;

e) Whilst building *C* shelters the court-yard, the access gap between buildings *C* and *D* allows high speed winds into the courtyard. This wind is deflected, first by building *B*, followed by building *C*, which results in a counter clockwise vortex due to the enclosed structure of the courtyard and experiences both windy and sheltered areas;

f) Finally, the length of building *A* creates a sheltering effect which creates a low speed wake wind behind it. Subsequently, this wake forms a flow separation at each end, with a large wake flow with two circulation zones in opposite directions.

Interestingly, this simulation shows that an urban form comprising only five buildings significantly alters the airflow direction and speed at various points throughout the complex. In summary, for a prevailing south wind (with different urban background wind directions), similar wind pattern characteristics have been observed: channelling of airflow, faster corner flows, circulating flows in sheltered zones and deflected flow at windward walls.

3.2 Simulation Case 2: Northerly Wind (N)

Figure 6 shows the simulated wind velocity vectors of the building complex, again at a height of 4 m above ground level. The observed airflow features are:

a) Diversion and separation of the northerly wind at frontal building *A* due to its oblique orientation;

b) Faster corner flows where the airflow separates, experienced at buildings *A* and *B*;

c) Circulation flows in the wake of buildings *C*, *D* and *F*;

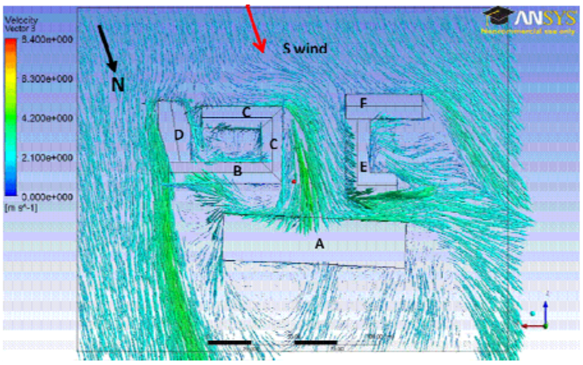

Figure 5. Simulation case 1: Southerly wind.

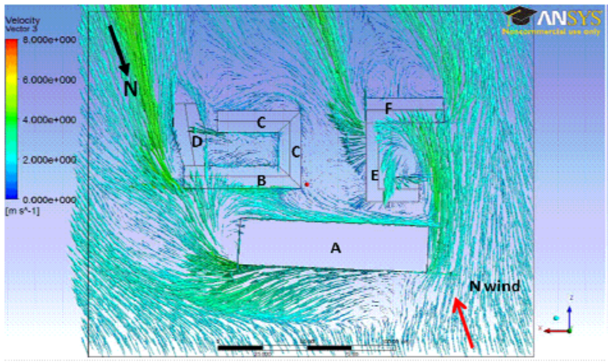

Figure 6. Simulation case 2: Northerly wind.

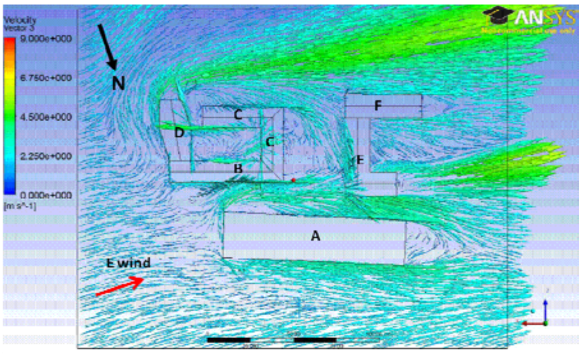

Figure 7. Simulation case 3: Easterly wind.

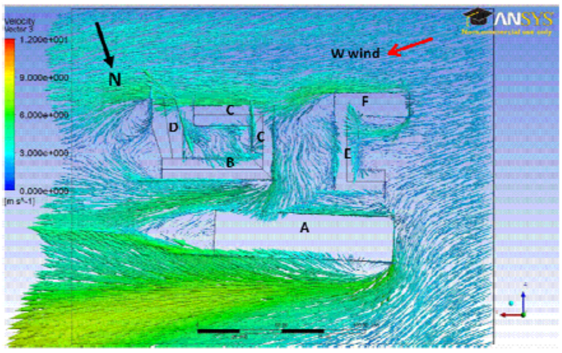

Figure 8. Simulation case 4: Westerly wind.

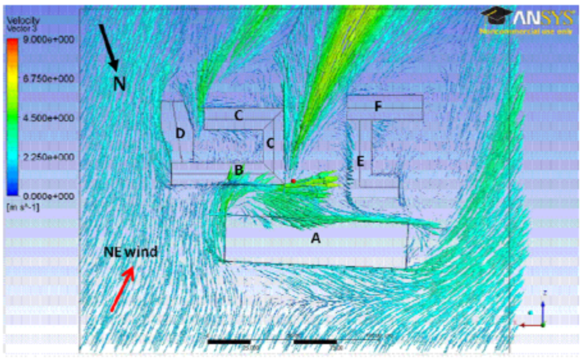

Figure 9. Simulation case 5: North easterly wind.

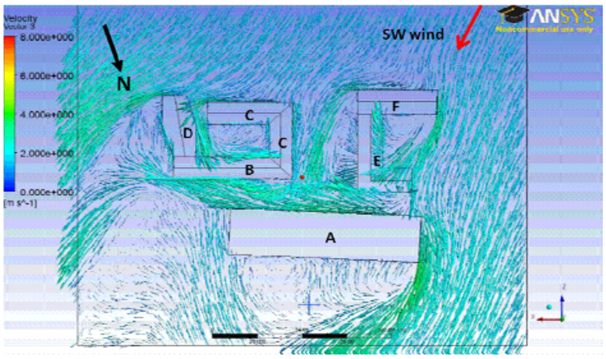

Figure 10. Simulation case 6: South westerly wind.

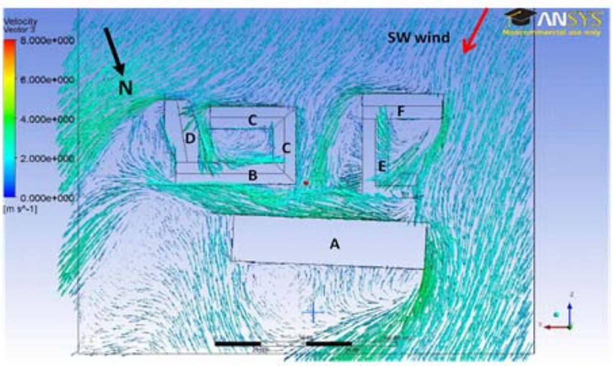

Figure 11. Typically low wind speed areas in a south westerly wind.

d) Calm wind situations in the courtyard because of no direct wind access;

e) Absence of wind channelling;

f) The 'U' shaped structure formed by buildings *E* and *F* create a counter clockwise vortex inside the semi open space. The slight protrusion of building *F* (relative to building *E*) appears to capture and divert air flow towards the semi closed space. Moreover, building *F* is taller than building *E* by approximately 4 m which allows a proportion of diverted wind flow over building *B*, thus creating higher wind speed at the front side of building *E*;

g) Whilst a southerly wind has created a large shelter zone behind building *A* (Figure 5), a northerly wind fails to create a low speed zone behind building *A* (Figure 6). This is largely due to the off-set position of building *B* relative to building *A*; building *B* also deflects north wind along the urban street canyon formed by buildings *A* and *B*, resulting in further wind migration towards the back of building *A*. This situation could be viewed as surprising, due to the considerable sheltering effect of building *A* which is the tallest building on the complex. However, its sheltering effect hugely influences the low wind speeds experienced between buildings *C* and *E*.

After examining the two opposing wind directions, it is clear that the effect of urban form, in terms of shape, size, orientation and relative positioning, determines microclimatic urban wind patterns.

3.3 Simulation Case 3: Easterly Wind (E)

Figure 7 shows simulation results for an easterly wind with velocity vectors given at a height of 4 m above ground level. The observable features are:

a) A blocking effect caused by building *D*, deflecting airflow southward. At the south end of building *D*, the corner flow re-directs wind back to the once easterly direction, initially accelerating it, until it reaches its original speed;

b) An interesting airflow pattern into the space between buildings *C* and *E* is formed, where the sheltering effect of building *C* creates a low speed wake flow in this space;

c) Channelling airflow into urban street canyon *AB* and *AE*. Street canyon *AE* is narrower than *AB*, thus it experiences increased wind speeds indicated by the densely packed flow lines. There are two circulation zones with low wind speeds at space *CE*, caused by wind deflection from buildings *E* and *F;*

d) A counter clockwise vortex in the courtyard.

3.4 Simulation Case 4: Westerly Wind (W)

Figure 8 shows simulation results from a westerly wind which has the greatest wind speeds on the complex. The observed features are:

a) Wake flow at the rear of building *D* which is recognizable by a pair of circulation zones flowing in the opposite directions;

b) Principal wind blockage from frontal buildings *F* and *E*, with a strong resulting airflow down the south facing wall of building *F*. This flow continues along the south side of the complex, experiencing two partial diversions; one at the corner of building *C*, where a deflecting flow is created down street canyon *CE*, and a partial diversion at the corner of building *D*, resulting in a counter clockwise vortex in the courtyard;

c) Two secondary street canyon flows; one at canyon *AB* which experiences greater airflow speeds due to two airflow sources in comparison to the other canyon flow *AE* which is narrower but with only one wind flow source

Having reported results on the cardinal directions, the following two simulation cases look at the inter-cardinal directions south west and north east

3.5 Simulation Case 5: North-Easterly Wind (NE)

Figure 9 shows simulation results from a north-easterly wind with airflow velocities at 4 m. The following features were observed:

a) Deflection of wind in three directions due to the orientation of buildings *D*, *B* and *A;*

b) A deflected westerly flow caused by the north faces of building *A* which, after acceleration caused by corner flow at the west end, returns back to the original north easterly wind direction;

c) Corner flow at the east end of building *A* which accelerates the wind speed towards building *B*, before being deflected again, creating high wind speeds along canyon *AB* and lesser speeds in canyon *AE;*

d) Deflected flow along the east face of building *D;*

e) Greatly reduced wind speeds around buildings *E* and *F* due to the sheltering effect of building *A;*

f) Minimal wind speeds in the courtyard;

g) Circulating and accelerated airflow in canyon *CE*, caused by deflection of buildings *B* and *E* and corner flow at corner *BC;*

3.6 Simulation Case 6: South-Westerly Wind (SW)

Lastly, Figure 10 shows simulation results for a south-westerly wind with velocities at 4 m above ground level. The following features are observed:

a) The overall orientation of the complex favours a south westerly wind which is characterized by a more uniform flow through the complex facilitated by urban street canyons *CE*, *AB* and *AE;*

b) A large sheltered zone at the rear and east side of building *A;*

c) Faster average corner airflows;

d) An anticlockwise circular wind flow in the courtyard, caused by the protrusion of building *D*;

e) A strong clockwise air flow circulation in the semi-open space created by buildings *E* and *F*, generated by the protruding section of building *E;*

3.7 Comparison with the Experimental Results

Experimental wind measurements at six locations within the building complex are compared with the wind simulation results at these locations (Table 3) for two tests: (i) easterly wind (Figure 7), and (ii) north easterly wind (Figure 9). The locations of measurements (1 to 6) are displayed in Figures 1 and 2. At each measurement location, an automatic weather station (Davis Wireless Vantage Pro2) was installed to a street lighting column at a height of 4 m. The microclimatic variables air temperature, wind speed and direction, air humidity and global solar radiation (the total value of the direct and diffused components on a horizontal surface) were measured at five minute intervals. For each weather station, the climatic measurements were remotely logged to a data logger, which was kept indoors. The accuracy of the integrated sensor suite (ISS) of the weather station for measuring each climatic variable is ± 0.56 °C for air temperature, ± 5% for the wind speed, ± 7 deg for the wind direction, ± 3% for the air humidity and ± 5% for the solar radiation.

For an easterly wind, the numerical results and experimental measurements are in close agreement at each location, except for Mast 4. This relatively broad agreement between the simulation results and the measurements is an encouraging factor for the validity of the urban wind simulations for this building complex. For a north-easterly wind, while close agreement is observed for Masts 4 and 6, simulation results are relatively faster at Masts 1, 2 and 5. Depending on the approaching wind

Table 3. Comparison of experimental and computational wind speeds.

7 March 2010, 11:00			**Easterly wind**			(Figure 7)
	Mast 1 *(m/s)*	Mast 2 *(m/s)*	Mast 3 *(m/s)*	Mast 4 *(m/s)*	Mast 5 *(m/s)*	Mast 6 *(m/s)*
Simulation	2.3 m/s	2.8 m/s	1.7 m/s	2.3 m/s	0.9 m/s	1.8 m/s
Experiment	2.2 m/s	2.7 m/s	1.8 m/s	1.8 m/s	0.9 m/s	1.8 m/s

12 December 2009, 12:00			**North-East wind**			(Figure 9)
	Mast 1 *(m/s)*	Mast 2 *(m/s)*	Mast 3 *(m/s)*	Mast 4 *(m/s)*	Mast 5 *(m/s)*	Mast 6 *(m/s)*
Simulation	3.3 m/s	5.2 m/s	0.5 m/s	0.8 m/s	1.3 m/s	1.4 m/s
Experiment	2.0 m/s	2.2 m/s	1.3 m/s	0.9 m/s	0.9 m/s	1.3 m/s

direction, discrepancy for the simulated results may be expected at some locations because it was assumed that there were no neighbouring buildings outside the simulated complex. In reality, however, there are several additional building blocks surrounding the complex of five buildings which was isolated for the flow simulation. As a result, the uniform wind-flow imposed at the simulation boundary conditions does not reflect the blockage/deflection effects of those surrounding buildings. This is clearly a factor in identifying the discrepancy between results. When simulation results are compared to experimental results, it is of great importance that the type of simulation boundary conditions is taken into account for qualifying any differences.

3.8 Implications for Natural Ventilation in Buildings

In the context of sustainable architecture, natural ventilation design (Stavrakakis et al, 2008), hybrid ventilation design (Lomas et al, 2007) and passive cooling (Giovani, 2011), are key design features for many new developments. Ventilation and cooling strategies commonly use weather station data, often provided by national databases, which usually characterize *general* wind patterns and wind speeds. As seen in simulation cases 1 to 6, a general incoming wind speed with uniform flow and magnitude 2 m/s, can result in wind speeds between 0.5 m/s and 5 m/s with a range of wind patterns due to the urban built form, characterized by building density, size, height, orientation and layout. Furthermore, other methods used to assess the availability of natural ventilation (Yao et al, 2009) similarly use weather station data in their models which can result in over estimating the capacity for natural ventilation. Fenestration placement must consider the statistical distribution of wind direction and speed, coupled with the full impact of the microclimate, namely the localized wind environment.

The prevailing wind direction in Reading is south-westerly (Figure 10), although in some months during the spring season, this shifts to north easterly (Figure 9). Building services engineers and architects, through CFD techniques or other analysis methods, can identify the potential for natural ventilation and adapt designs as required to maximize the potential for passive ventilation and cooling. Extensive fenestration placement in locations, identified by the circular points in Figure 11, may not result in effective design for single sided ventilation, unless compensated by other strategies. On the other hand, for a cross-ventilation strategy, these circular points indicate the most favorable locations for fenestration placement. In reality, the wind resource in these locations would be even less than the simulated values, due to additional airflow turbulence upstream (south west) caused by neighbouring buildings and foliage. For example; in simplistic terms, one national database (DECC, 2011) quotes an average annual wind speed of 4.7 m/s (at 10 m above ground level) for Reading, UK, whereas in reality the study shows that incoming wind speeds are significantly reduced in many locations within the building complex.

In the street canyon, Building *B* benefits from a cross-ventilation strategy because Building *B* is also exposed to a low wind zone in the courtyard for most wind directions (except for SW wind). However, Building *A* only benefits from cross ventilation for S and SW winds. Since the courtyard is mostly a low wind zone, Buildings *B, C* and *D* benefit from cross-ventilation, in turn depending on wind direction approaching the exposed sides of these buildings.

4 Conclusions

Three-dimensional urban wind patterns were simulated using CFD for a building complex of six buildings which represent the following urban forms: street canyon, semi-closure and courtyard. These numerical results were validated by comparing them with experimental measurements at six representative locations within the site. The characteristic wind patterns of these three urban forms and their impact on each other were determined for six different wind directions. Depending on the predicted urban wind patterns in these urban forms, their impact on the natural ventilation of the building complex were discussed.

This study showed that urban form, characterized by building density, size, height, orientation and layout, significantly impacts on the local wind pattern and creates considerable variation in wind speed around building complexes. There are numerous implications for urban form on the design and management of natural and hybrid ventilation and cooling strategies. The underlying implication being that ventilation strategies based on weather station wind data have a propensity to over-estimate the amount of wind available for natural ventilation, which can result in under-performing cross, displacement and stack ventilation systems that may have to be retrospectively corrected. Subsequent correction procedures are often disruptive, costly, and cause excessive carbon emissions relative to the initial design assessment.

In addition to problems associated with ventilation, oversights in town planning can often result in pedestrians experiencing unexpected high winds at street level, which fail to match regional wind reports. A similar phenomenon also occurs for typical building layouts and open spaces. In particular, this study highlights the following airflow characteristics for such an urban form;

a) Channelling of airflow by parallel buildings;

b) Blockage and deflection of local wind by frontal lateral buildings;

c) Accelerated airflow at building corners during flow separation;

d) Sideways deflection of an oblique wind along the windward elevation of a building;

e) Achieving an exclusive sheltered zone at the rear of a building may be impossible due to close proximity buildings.

It is therefore crucial that urban wind patterns are correctly anticipated during the design stage of buildings and ventilation systems, and for town planning in general. CFD is suitable for this type of analysis and can help inform decisions that impact upon occupant and pedestrian comfort, as well as facilitate sustainable architectural principles such as passive cooling and natural ventilation.

Acknowledgements

The authors would like to thank the UK Engineering Physical and Science Research Council (EPSRC EP/F039867/1) and the project steering committee members Hywel Davies and Anastasia Mylona from the Chartered Institution of Building Services Engineers (CIBSE), Bill Watts from Max Fordham, David Hughes from MTT Consulting, Alan Short from Short and Associates, Tony Day from London Southbank University, and Derek Clements-Croome and Hazim Awbi from the University of Reading. The authors would also like to thank Jing Liu, Sohrab Donyavi, Yafeng Gao for their assistance in data collection.

References

Branis M, Hovorka J, Rezacova P, Domasova M and Lazaridis M: (2005) "Effect of indoor and outdoor sources on particulate matter concentration in a naturally ventilated flat (URBAN-AEROSOL Project Prague)". *Indoor and Built Environment*. **14**, pp 307-312.

Chen Q: (2004) "Using computational tools to factor wind into architectural environment design". *Energy and Building*. **36**, pp1197-1209.

CLG: (2006) "Code for Sustainable Homes. A step-change in sustainable homes building practice". Department for Communities and Local Government, UK.

DECC: (2011) "Wind speed database". Department of Energy and Climate Change (DECC) Available at: http://www.decc.gov.uk/en/content/cms/meeting_energy/wind/windsp_databas/windsp_databas.aspx [accessed 29/10/11].

Fung WY, Lam KS, Hung WT, Pang SW and Lee YL: (2006) "Impact of urban temperature on energy consumption of Hong Kong" *Energy*, **31**, pp2623-2637.

Giovani B: (2011) "Indoor temperature reduction by passive cooling". *Solar Energy*. **85**, 8, pp1692-1726.

Jiang Y, Xing H, Straub C, Chen Q, Scott AM, Glicksman LR and Nonford LK: (2007) "Design of natural ventilation and outdoor comfort by a team of architects and engineers with the CFD technique". Sustainable Urban Housing in China. MIT Building Technology Group, Cambridge MA 02139 USA.

Kolokotroni M, Giannitsaris I and Watkins R (2006) "The effect of the London urban heat island on building summer cooling demand and night ventilation strategies". *Solar Energy*. **80**, pp383-392.

Lomas KJ, Cook MJ and Fiala D: (2007) "Low energy architecture for a severe US climate: Design and evaluation of a hybrid ventilation strategy". *Energy and Buildings*. **39**, pp32-44.

Memon RA and Leung DYC: (2010) "Impacts of environmental factors on urban heating". *Journal of Environmental Sciences-China*. **22**, pp1903-1909.

Nakamoura Y and Oke TR: (1967) “Wind, temperature and stability condition in an E-W oriented urban canyon”. *Atmospheric Environment*. **22**, pp2691-2700.

Oke TR: (1988) “Street design and urban canopy layer climate” *Energy and Buildings*. **11**, pp103-113.

Ghiaus C and Allard F: (2005) “Natural ventilation of urban buildings- summary of URBVENT project” *International Conference Passive and Low Energy Cooling for the Built Environment*”, May 2005, Santorini, Greece, pp29-33.

Priyadarsini R, Hien WN and David CKW: (2008) “Microclimatic modeling of the urban thermal environment of Singapore to mitigate urban heat island”. *Solar Energy*. **8**, pp727-745.

Rostron J: (1998) “Sick Building Syndrome – Concepts issues and practice”. Spon Press, London.

Serteser N and Ok V: (2009) “The Effects of Building Parameters on Wind Velocity and Air-Flow Type in the Urban Settlements” *The Seventh International Conference on Urban Climate, Yokohama, Japan 29 June-3 July.*

Stavrakakis, GM, Koukou MK, Vrachopoulos MGr and Markatos NC: (2008) “Natural cross-ventilation in buildings: Building-scale experiments, numerical simulation and thermal comfort evaluation”. *Energy and Buildings*. **40**, pp1666-1681.

Turkbeyler E and Yao R: (2009) “ Experimental study of urban microclimate for a building complex”. *The International Conference in Sustainable Development in Building and Environment, Chongqing, China 28-30 October.*

Turkbeyler E, Yao R and Day T: (2011) “Urban microclimates and renewable energy use in cities”. *World Renewable Energy Congress, Linkoping, Sweden, 8-13 May.*

Vaughan S, Paul G, David M and Craig W: (2002) “The relationships between indoor and outdoor respirable particulate matter: Meteorology, chemistry and personal exposure”. *Indoor and Built Environment*. **11**, pp266-274.

Yang L and Li Y: (2011) “Thermal conditions and ventilation in an ideal city model of Hong Kong”. *Energy and Buildings*. **43**, pp1139-1148.

Yao R, Li B, Steemers K and Short A: (2009) “Assessing the natural ventilation cooling potential of office buildings in different climate zones in China”. *Renewable Energy*. **34**, pp2697-2705.

Zhang YW, Gu ZL, Lee SC, Fu TM and Ho KF: (2011) “Numerical simulation and in situ investigation of fine particle dispersion in an actual deep street canyon in Hong Kong”. *Indoor and Built Environment*. **20**, pp206-216.